Nonlinear Response of Ozone to Precursor Emission Changes in China: a Modeling Study using Response Surface Methodology

J. Xing[1], S.X. Wang[1], C. Jang[2], Y. Zhu[3], J.M. Hao[1, *]

1 Department of Environmental Science and Engineering, and State Key Joint Laboratory of Environment Simulation and Pollution Control, Tsinghua University, Beijing 100084, CHINA

2 The U.S. Environmental Protection Agency, Research Triangle Park, NC 27711, U.S.A.

3 School of Environmental Science and Engineering, South China University of Technology, Guangzhou 510006, CHINA

Abstract

Statistical response surface method (RSM) is successfully applied in Community Multi-scale Air Quality model (CMAQ) analysis on ozone sensitivity studies. Prediction performance has been validated through cross validation, out of sample validation and isopleths validation. Sample methods and key parameters including the maximum numbers for variables involving in statistic interpolation as well as training sample number have been tested and selected through computational experiments. Overall impacts from individual sources including local/regional NOx and VOC emission sources and NOx emissions from power plants for three megacities as Beijing, Shanghai and Guangzhou have been evaluated through RSM analysis under a July 2005 modeling study. NOx control appears to be beneficial for ozone reduction in the downwind areas where usually have higher ozone levels, and it's likely to be more effective than anthropogenic VOC control during heavy photochemical pollution period. Regional NOx sources are strong contributors to surface ozone mixing. Local NOx emission control without regional involvement may bring the risk of increasing urban ozone levels due to the VOC-limited conditions, but it gives considerable control benefit for ozone in upper layers (up to 1 km, where the ozone chemistry is changed to NOx-limited condition) and helps to improve regional air quality in the downwind areas. Stricter NOx emission control has higher effects on ozone reduction because of

* Corresponding author. Tel: 86-10-62782195
E-mail address: hjm-den@tsinghua.edu.cn

the shift from VOC-limited regime to NOx-limited regime. Therefore, NOx emission control should be significantly enhanced to reduce the ozone pollution in China.

Keywords

Ozone control, Air quality model, Photochemical model, Ozone sensitivity analysis, Response Surface Model, NOx and VOC Emissions

1 Introduction

Tropospheric ozone is not only a key air pollutant that affects human health, crop productivity and natural ecosystems, but also a greenhouse gas that affects global climate. During the past two decades, the rapid economic growth in China has resulted in a significant increase in the emissions of ozone precursors such as nitrogen oxides (NOx) and volatile organic compounds (VOC) (Ohara et al., 2007; Wei et al., 2008; Zhang et al., 2009a). The large emissions lead to the formation of elevated ozone over urban and downwind suburban areas. High ozone concentrations over 200 μg m^{-3} (approximately 103 ppb, the 1-hour maximal concentration defined by National Ambient Air Quality Standard of China, Class II) have been frequently observed by in-situ monitoring in east China in recent years (Shao et al., 2006; Wang et al., 2006a, b. c; Zhang et al., 2008; Tang et al., 2009; Tie et al., 2009; Ran et al., 2009; Shao et al., 2009).

Effective attainment of ground-level ozone standards depends upon the reliable estimation of ozone responsiveness to controls of its precursor emissions (Cohan et al., 2006, 2007). In general, ozone formation is classified into two categories of chemical regimes, NOx-limited and VOC-limited regimes. In the NOx-limited regime, ozone increases with increasing NOx and exhibits only slight sensitivity to VOC; in the VOC-limited (or NOx-rich) regime, ozone increases with increasing VOC and exhibits slight or even negative sensitivity to NOx. Transitional conditions of dual sensitivity also occur. Classification of ozone production regime helps determine whether NOx or VOC emissions should be targeted more aggressively in strategies to reduce ozone. However, ozone responsiveness is challenging to simulate due to the spatial/temporal variations of

precursor emissions and meteorological conditions (Seinfeld and Pandis, 2006).

Indicators such as NOy, H_2O_2/HNO_3 and $H_2O_2/(O_3+NO_2)$ simulated by air quality model are used to define the ozone chemistry in a number of studies (Sillman et al., 1995; Tonnesen et al., 2000; Zhang et al., 2009b). Air quality models (AQMs) can be a powerful regulatory tool for comparing the efficacy of various emissions control strategies and policy decisions. Advanced tools embedded in AQMs including ozone source apportionment technology (OSAT) (ENVIRON, 2002; Dunker, et al. 2002; Xu et al., 2008; Wang et al., 2009), process analysis (PA) (Jang et al., 1995; Zhang et al., 2005, 2009; Liu et al., 2010), direct decoupled methods (DDM) and high-order decoupled direct method (HDDM) (Dunker et al, 2002; Hakami et al, 2003; Cohan et al., 2005) enable a better understanding of ozone formation mechanisms. However, due to the often enormous computational costs and the complication of the required emission inputs and processing, using complex air quality models to generate outputs to meet time-pressing requirements of policy analysis always presents a challenge and is typically inefficient, if not ineffective. A promising tool for addressing this issue, Response Surface Methodology (RSM), has been developed by utilizing advanced statistical techniques to characterize the relationship between model outputs and input parameters in a highly economical manner. The RSM is a metamodel of air quality model. It is a reduced-form prediction model using statistical correlation structures to approximate model functions through the design of complex multi-dimension experiments. The RSM technique has recently been successfully tested and evaluated for a series of $PM_{2.5}$ and ozone assessments and policy analyses in the United States (US EPA, 2006a, b).

In this paper, we develop a response surface model with Community Multi-scale Air Quality (CMAQ) (Byun and Schere, 2006) simulations to investigate ozone sensitivities to NOx and VOC emission changes in east China during a summer month. The performance of response surface model is validated by additional CMAQ simulations, referred to as out of sample validation, and leave-one-out cross validation. Ozone chemistry in spatial and temporal scale is identified when

the precursor emissions change from 0% to 200%. Ozone reduction effectiveness is evaluated when different control measures applied to different sectors in three mega-cities as Beijing, Shanghai and Guangzhou. Synchronized strategies to attain ozone national standards are also discussed.

2 Methodology

The processes involved in developing the ozone RSM application using CMAQ include the selection of modeling domain and configuration, development of multi-dimension experimental design for control strategies, and implementation and validation of the RSM technique, as shown in Fig.1.

2.1 Emission inventory

Emissions of SO_2, NO_x, PM_{10}, $PM_{2.5}$, BC, OC, NH_3, and NMVOC were calculated based on the framework of the GAINS-Asia model (Amann et al., 2008). The general method used to develop the China regional emission inventory is described in our previous paper (Klimont et al., 2009). To improve the emission estimates, data for emission factors were collected from field measurements performed by Tsinghua University and other published sources in China. A unit-based methodology is applied to estimate emissions from large point sources including coal-fired power plants, iron and steel plants, and cement plants (Zhao et al., 2008; Lei et al., 2008). Detailed local emission information aggregated from the bottom-up investigation of individual power plants, heating boilers, and industries in Beijing (BJ), Yangtze River Delta (YRD) and Pearl River Delta (PRD) are also incorporated into the national emission inventory (Li et al., 2008; Zheng et al., 2009; Wang et al., 2010b). The national emissions in 2005 are summarized in Table 1. The anthropogenic emissions of SO_2, NO_x, PM_{10}, $PM_{2.5}$, BC, OC, NH_3 and NMVOC in China were 28651kt, 18499kt, 19237kt, 14245kt, 1595kt, 3494kt, 16556kt, and 19406kt, respectively. Compared to other ones available in literature, e.g. Streets et al. (2003), Zhang et al. (2009), the uncertainties in our base year emissions are relative lower. The uncertainties (i.e., 95% confidence

intervals around the central estimates) of NOx and VOC emission inventory used in this study are -10%~36% (Zhao et al., 2010) and -44%~109% (Wei et al., 2008).

2.2 MM5/CMAQ modeling domain and configuration

The air quality model used to develop response surface model is CMAQ modeling system (ver. 4.7), developed by the US EPA (Byun and Schere, 2006). A one-way nested technique is employed in this study. Modeling domain 1 covers almost entire China with a 36×36 km horizontal grid resolution and generates the boundary conditions for nested domain at 12-km resolution over popular Eastern China (domain 2), as shown in Fig. 2(a). Three sub-areas (i.e., Beijing, YRD and PRD) within domain 2 are selected for analysis. The vertical resolution of CMAQ includes fourteen layers from the surface to the tropopause with denser layers at lower altitudes to resolve the planetary boundary layer (PBL). The Carbon Bond Mechanism (CB05) with aqueous and aerosol extensions and the AREO5 aerosol mechanism are chosen for the gas-phase chemistry and aerosol modules, respectively. A spin-up period of six days is used for model simulations to reduce the influence of initial conditions on model results. The CMAQ simulation period is the entire month of July 2005. A complete description of CMAQ, meteorological, emission, and initial and boundary condition inputs used for this analysis are discussed in Xing et al. (2010) and Wang et al. (2010a). The CMAQ simulations of this modeling system have been validated through comparison with observations of satellite retrievals and surface monitoring data. We compared the simulated ozone concentration with the observed data of six monitoring stations in Beijing, including five urban sites, as Qianmen, Dongsi, Tiantan, Aoti, Nongzhanguan, Gucheng, and one rural site as Dingling, which were described in Streets, et al. (2007) and Wang et al. (2008). The normalized mean bias of simulated hourly ozone concentration during 8:00am-8:00pm (Beijing time) is 9%, with related coefficient as 0.76. Additionally, the performances of CMAQ simulation on ozone concentration with the same bottom-up emission inventories have been validated by Li et al. (2008) for Yangtze River Delta in January and July 2001, and Wang et al. (2010b) for Beijing in July and August 2008.

2.3 RSM experiment design

RSM uses statistical techniques to build response relationships between a response variable (in this case ozone concentration in this study) and a set of control factors of interest, e.g. emissions of precursor pollutants from particular sources and locations, through designed experiments (Box and Draper, 2007). RSM is a meta-model built upon multi-"Brute Force" model simulations, which can help avoid the uncertainties from the systematical complexity. Due to the limitation of computational capability, design of good experiments is the key issue to build reliable responses with limited samples (Santner et al., 2003), and it is requisite to ensure the accuracy of prediction model. Most of previous studies on O_3 control analyses explored the overall impacts of two factors (total NOx and total VOC emission) on ozone that may be successfully derived from statistical interpolation of dozens training samples (Milford et al., 1989; Shih et al., 1998; Fu et al., 2006), the interpolation is much more complicated when the precursor emissions are separated by pollutants, sectors and regions (Wang and Milford, 2001). Constraints are placed on the experimental design space, i.e. the region over which the response is studied, to a set of variables that parameterize a set of possible emissions control strategies, and evaluate the change in ambient ozone levels that result from a change in emissions.

Selection of policy factors were based on precursor emission type and source category relevant to policy analysis of interest. The experimental design carefully considered factors that would provide maximum information for use in comparing relative efficacy of different emissions control strategies. To develop independent response surfaces for particular urban areas, as well as a generalized response surface for all other locations (outside of the particular urban areas), we applied a regional design for the RSM experiment. In this study, the particular cities selected are Beijing, Shanghai and Guangzhou. Local versus regional impacts have been teased out for the three cities. The local emissions in those three cities are grouped together as one region (Region A), and the other areas are grouped as another region (Region B). In our analysis, Region A represents the

local emission of each city. To testify the independence of three cities, sensitivity analysis was conducted to calculate the impact of one city's emission on the other two, which is given by the differences between the baseline simulation and the controlled simulation which zeroed out all emission in selected cities, as shown in Fig. 2b. The Fig. 2b gives the influence scope of three cities. It can be seen that the interactions of their emission impacts are less than 0.5 ppb, which is negligible. Thus, selection of these areas allows the RSM to analyze air quality changes in these 3 urban areas independent of one another. On a local or regional basis, the ozone precursor emissions are categorized into NOx emission from power plants (POW, represents point sources in higher layers), NOx emission from other area sources (OTH, represents area and mobile sources at the surface layer), and VOC emissions, as shown in Table 2. We defined "emission ratios" as the ratio of the changed emissions compared to the baseline emissions. For example, the "emission ratio" is 1 for baseline emissions, and the "emission ratio" is 0.6 for 40% emission reduction.

Table 2 gives the sampling method and numbers of training sample used during ozone response surface model development. Method as Hammersley quasi-random Sequence Sample (HSS) (Hammersley, 1960) which could quickly "fill up" the space in a well-distributed pattern with low discrepancy are adopted in this study. Besides, we choose Latin Hypercube Sample (LHS) (Iman et al., 1980), a widely-used (Wang and Milford, 2001; US EPA, 2006a, b) filling method which ensures that the ensemble of random samples is good representative of the real variability, as an optional choice (Fig. 3a). Based on the uniform-distributed LHS/HSS which has the relative equiprobable interval over the range, additional margin processing is conducted to improve the performance of prediction at margins. Here we choose power function to apply on the samples from uniform-distributed LHS/HSS, as follows:

$$TXn = \begin{cases} X, & n = 1 \\ \left(\frac{X-a}{b-a} \times 2\right)^n \times (b-a) + a, & X \le a + \frac{b-a}{2}, n > 1 \\ \left[1 - \left(\frac{b-X}{b-a} \times 2\right)^n\right] \times (b-a) + a, & X > a + \frac{b-a}{2}, n > 1 \end{cases} \quad \text{(E1)}$$

Where X is sampled from uniformed LHS/HSS in section [a, b] (in this study we choose [0, 2], which means the emission changes are from all-controlled to be-doubled); TXn is the samples after margin process; n is the order indicting the marginal level.

Another purpose of margin processing is to sample more possible situations. Normally we assume the variables have no direct interaction among each other, however, the variables considered in such predict system are related, e.g., total VOC = VOC from local sources (variable a) + VOC from regional sources (variable b). Samples generated by uniformed methods would provide even distributions for individual source, but non-even for the total emission (here as total VOC) with less samples located in the marginal areas and its density of distribution followed as N (represent the number of pollutant sources) power function, as shown in Fig. 3b. Therefore, margin process is used to enlarge the sample density located in the marginal areas. The optimized marginal level n is selected through computational tests during preliminary experiments (see details in section 3.1.2).

In case LHS1-30, we can simply use 30 training samples generated by LHS method to map the ozone mixing ratios vs. total-NOx and total-VOC emission ratios. In the case of HSS6-200, 4 types of NOx emission sources and 2 VOC emission sources are involved, the number of training samples and optimized marginal levels are determined according to the results of preliminary experiments, as shown in Fig. 1 (orange lines). Due to the expensive computational cost of hundreds of CMAQ simulations, we adopt the "quasi-response" of ozone to precursors' emissions based on statistical calculation during preliminary experiments.

The "quasi-response" is based on the results of LHS1-30. Since total emission is the sum of individual emission sources, the emission ratio of total emission is the weighted mean of the

emission ratios of each emission source:

$$tNOX = \sum_{i=1}^{m} NOX_i, \quad R-tNOX = [R-NOX_1, \cdots, R-NOX_m] \bullet A^{m\times 1} \tag{E2}$$

$$tVOC = \sum_{j=1}^{n} VOC_j, \quad R-tVOC = [R-VOC_1, \cdots, R-VOC_n] \bullet B^{n\times 1} \tag{E3}$$

where $tNOX$ and $tVOC$ are respectively total NOx emissions and total VOC emissions; NOX_i and VOC_j is emission of each individual source; $R-tNOX$ and $R-tVOC$ are respectively the emission ratio of total NOx emissions and total-VOC emissions; $R-NOX_i$ is the emission ratio of NOx emission from source *i*; $R-VOC_j$ is the emission ratio of VOC emission from source *j*; $A^{m\times 1}$ and $B^{n\times 1}$ are the weight coefficients for each NOx and VOC sources. The "weight coefficient" reflects contribution from each emission source, which is defined by the following equations. $NOX_i = tNOX \times A(i)$, $tNOX = \sum_{i=1}^{m} NOX_i = \sum_{i=1}^{m} tNOX \times A(i)$; In the preliminary experiments, the "weight coefficients" (A(1), A(2)…A(n)) were set to be 1:2:3..:N, with sum as 1. One should be noted that such assumption is not always valid, since the long-range transports of regional emissions and large point sources would give different impacts. Such assumption allows us to explore the sensitivity of crucial parameters to the prediction bias through hypothetical computational testing efficiently (see details in section 3.1.2).

2.4 Statistical and prediction method

Each training sample represents one emission control scenario which is simulated by CMAQ and then used for RSM. Based on those simulated ozone responses, RSM prediction system are statistically generalized by MPerK (MATLAB Parametric Empirical Kriging) program followed Maximum Likelihood Estimation - Experimental Best Linear Unbiased Predictors (MLE-EBLUPs) (Santner et al., 2003). The calculation is based the following equation:

$$\vec{Y}\left(x_0\right)=\vec{Y}_0=\sum_{j=1}^{d} f_j\left(x\right)\vec{\beta}_j+Z\left(x\right)\equiv f_0^T\vec{\beta}+\vec{\gamma}_0^T\vec{R}^{-1}\left(Y^n-F\vec{\beta}\right) \quad \text{(E4)}$$

Where $\vec{Y}\left(x_0\right)$ is the predicted concentration from RSM; f_0 is the $d\times 1$ vector of regression functions for Y_0^n; F is the $n\times d$ matrix of regression functions for the training data; $\vec{R}$ is the $n\times n$ matrix of correlations among the Y^n; $\vec{\gamma}_0$ is the $n\times 1$ vector of correlations of Y^n with Y_0^n; $\vec{\beta}$ is the $d\times 1$ vector of unknown regression coefficients and the generalized least squares estimator of $\vec{\beta}=\left(F^T\vec{R}^{-1}F\right)^{-1}F^T\vec{R}^{-1}Y^n$.

The Product Power Exponential correlation is chosen as the correlation functions for prediction:

$$R\left(h\middle|\xi\right)=\prod_{i=1}^{d}\exp\left[-\theta_i\left|h_i\right|^{p_i}\right] \quad \text{(E5)}$$

Where $\xi=\left(\theta,p\right)=\left(\theta_1,...,\theta_d,p_1,...p_d\right)$ with $\theta_i\geq 0$ and $0<p_i\leq 2$, the ξ estimator is the maximum likelihood estimate (MLE).

In order to confirm the reliability of RSM reproducing CMAQ simulations, the above prediction method is validated through "leave-one-out cross validation" (LOOCV), out of sample validation and 2-D isopleths validation. The definition of LOOCV is to use a single sample from the original datasets as the validation data, and the remaining sample as the training data to build prediction RSM. Each sample in the datasets is used once as the validation data. For example, for N training data (d1, d2…dN), the sample i (di) has been selected as the validation data, and the remaining samples (d1, d2…d(i-1), d(i+2)…dN) are used to build RSM to predict the sample i and make comparison. Out of sample validation needs additional CMAQ cases which are not included in training samples, then RSM predictions are compared with those extra CMAQ simulations. Validation of 2-D isopleths compares the prediction results of 2-D isopleths with that of multi-dimension RSM system, which is used to evaluate the stability of RSM system with higher

dimensions.

Point-to-point data are compared through correlation analysis and error analysis. The correlation coefficient (R) and Mean Normalized Error (MNE) are calculated through following equations:

$$R = \sqrt{\frac{\left[\sum_{i=1}^{N}\left(M_i - \overline{M}\right)\left(O_i - \overline{O}\right)\right]^2}{\sum_{i=1}^{N}\left(M_i - \overline{M}\right)^2 \sum_{i=1}^{N}\left(O_i - \overline{O}\right)^2}} \quad \text{(E6)}$$

$$MNE = \frac{1}{N}\sum_{i=1}^{N}\frac{\left|M_i - O_i\right|}{O_i} \quad \text{(E7)}$$

Where M_i and O_i are the RSM predicted and CMAQ simulated value of the ith data in the series (temporal or spatial); and $\overline{M}$ and $\overline{O}$ are the average simulated and observed value over the series.

3. Results and Discussion

3.1. Development and validation of RSM-Ozone system

The results of RSM modeling case LHS1_30 (as shown in Table 2) were used as "quasi-response" in preliminary experiments. The results of modeling case HSS6_200 (as shown in Table 2) were compared with that of LHS1_30 through leave-one-out cross validation, out-of-sample validation and 2-D isopleths validation. Sensitivity analysis was conducted to check the RSM prediction performance to the marginal level, sample numbers, and variable numbers.

3.1.1 Validation of RSM performance

Using the LOOCV method, the ozone levels simulated by CMAQ and predicted by RSM are compared for both case LHS1-30 (31 pairs of data) and case HSS6-200 (201 pairs of data), as shown in Fig. 4. Strong linear relationship (y=x) between CMAQ and RSM datasets are found in all areas for both cases, with square of R are larger than 0.99. For Beijing, Shanghai, Guangzhou

and East China, the mean normalized errors (NE) of LHS1-30/HSS6-200 are respectively 0.2%/0.6%, 0.4%/0.6%, 0.9%/0.5%, and 0.3%/0.2%, and the maximum NEs are respectively 1.5%/4.1%, 2.7%/8.3%, 6.0%/5.5%, and 1.6%/1.8%. These results suggest that RSM prediction gives pretty good performance for all levels of ozone mixing ratio in both LHS1-30 and HSS6-200 cases.

Extra CMAQ simulations with certain NOx and VOC emission ratios, as seen in Table 3, have been conducted to validate the RSM prediction. For Beijing, Shanghai, Guangzhou and East China, the mean NEs of LHS1-30/HSS6-200 are respectively 1.9%/1.2%, 0.7%/0.4%, 0.5%/0.5% and 0.5%/0.6%, and the maximum NEs of LHS1-30/HSS6-200 are respectively 3.9%/3.5%, 1.8%/2.0%, 1.8%/5.5% and 1.6%/1.8%. These results indicate that the RSM predictions are with good accuracy compared to CMAQ simulations, though relative larger biases occurred for low ozone mixing ratios.

The 2-D isopleths of Ozone responses to the emission changes of total NOx and total VOC in HSS6-200 are given in Fig. 5(a). From Fig. 5(a), we can see the strong non-linear response of ozone to precursors' emissions in the three megacities. RSM is able to reveal such non-linear relationship between the responses of ozone concentrations to the changes precursors' emissions in an efficient and reliant way. The 2-D isopleths of NE, as shown in Fig. 5(b), represents the differences between LHS1-30 and HSS6-200. The errors are below 1%. When NOx emissions ratios are below 0.4 (60% of NOx emissions reduced), larger NEs (2~15%) are found because of the marginal effects. Besides, the NOx/VOC emission ratios corresponding to the inflection points are consistent in both LHS1-30 and HSS6-200. That confirms the stability of RSM with high dimensions (HSS6-200).

3.1.2 Sensitivity of RSM predictions to key parameters

As we discussed in section 2.2, the optimized marginal level (n) are determined through computational experiments with "quasi-response" built in section 2.3. Test samples are defined as

all NOx and VOC changes from 0.0 to 2.0 stepped by 0.1 respectively, total 441 pairs in all. Sensitivities of prediction performance to the marginal level are shown in Fig. 6. Six variables including 4 NOx sources and 2 VOC sources are involved, sampled by two methods as LHS and HSS. In quasi-HSS-4vs2 (4 types of NOx with 2 types of VOC sources, 100~160 samples), obvious improvement of prediction performance is found after marginal processing. Similar improvement is found in quasi-LHS-4vs2 (4 types of NOx with 2 types of VOC sources, 160 samples), with level 3~4 marginal processing. The MNEs are reduced by 50%, from 8% to 3%.

In order to explore the sensitivity of prediction performance to numbers of samples and variables, we conduct a series of computational experiments with different variable and sample numbers using both LHS and HSS with marginal processing, as seen in Fig. 7. To obtain good prediction performance with MNE < 1% and R>0.99, cases with few variable numbers such as 2(1vs1) and 4(2vs2) need small number of training samples (<30 for 2(1vs1) and <60 for 4(2vs2)). Errors increase along with the increase of variables. When the variable numbers are 6(4vs2) and the sample number are over 150, the MNEs are still within acceptable range (<2%) and correlation coefficient (R) is over 0.99. However, when variable numbers are 8(6vs2) and 10(8vs2), MNEs are increased to 5% and 7% and correlation coefficient are decreased to 0.8 and 0.5, respectively. Increasing of sample numbers can not reduce the errors caused by the increase of variables, since the sample space is sharply enlarged with the increase of dimensions. That indicates there is a risk of statistics failure. Number of variables is the most crucial parameter that should be determined through computational experiments before one RSM case is established.

3.2. Application of ozone RSM in Beijing, Shanghai and Guangzhou

3.2.1 Identification of ozone chemistry

In the isopleths of ozone response to changes of precursor emissions predicted by RSM, the NOx emission ratio at the peak ozone concentrations under baseline VOC emissions is defined

as peak ratio, or ridge line ratio. When peak ratio is lower than current NOx emission ratio (baseline emission ratio = 1), the control of NOx emissions may not effectively reduce ozone levels. When peak ratio is higher than current NOx emission ratio, the control of NOx emissions will effectively reduce ozone levels. Use of peak ratio as an index will not only help to identify the status of ozone response regime, but also indicate how much NOx emission reduction may be needed to avoid the potential negative impacts on ozone reduction. We also compared the spatial distribution of NOy mixing ratio with that of peak ratio.

Due to the spatial variations of precursor concentrations, the ozone response varies in different locations (Xu et al., 2008). The spatial distributions of ozone concentrations, NOy concentrations and peak ratios over three selected urban areas are shown in Fig. 8. The areas with peak ratio values less than 1 are mainly located in the city center in Beijing, Shanghai, Guangzhou, as well as Tianjin (in south of Beijing) and Hong Kong, due to the high density of NO_2 resulted from local emission sources. The spatial distributions of NOy mixing ratio and peak ratio are consistent in all 3 regions. That suggests that peak ratio is as good as NOy, but peak ratio further serves an indicator for the degree of NOx emissions needed to be reduced to become NOx-limited from VOC-limited, which can be very important for designing urban ozone control strategy.

High ozone concentration usually appears in downwind rural areas such as the north of Beijing and Guangdong, rather than the city centers. The peak ratio changes from 0.8 to 1.2 along with the distance from city center. Similarly, NOy mixing ratio changes from 20ppb to 5ppb. These results indicate that NOx control is beneficial to ozone reduction in the downwind areas which usually have higher ozone mixing ratios than urban areas.

The ozone response varies with vertical height as well. The vertical profiles of peak ratio values and ozone mixing ratios in 3 cities are shown in Fig. 9. The peak ratio is lower than 1 in the surface layer of 3 cities. Therefore it is hardly seen the benefit of 70% NOx reduction on ozone pollution in surface layer. While above layer 3~6 (vertical height 72~674 meters), the peak ratio

values are higher than 1, which indicates the strong benefits of NOx control on ozone reduction. We can see the ozone responses when NOx emission is reduced 50%~70%. Although the controls of NOx emissions may not provide reduction of urban local ozone levels, it can reduce the downwind transport of ozone, and thus the benefit for regional air quality can be significant.

Due to the variation of in-situ meteorological conditions, including temperature, humidity, sunlight radiation density, as well as wind speed and precipitation, the ozone chemistry varies significantly in temporal scale. Large differences are found in the comparison of averaged ozone isopleths for high ozone days (>70ppb) and lower ozone days (<30ppb) in three cities, see in Fig. 10. During the days when higher ozone (>70ppb) occurs under favorable meteorological condition for photochemical production of ozone, the ozone response is mostly NOx-limited, with peak ratio larger than 0.8. The NOx emission control is benefit for Ozone reduction. However, in the days with lower ozone mixing ratio (<30ppb), usually the effects of NOx controls are negative for ozone, with peak ratio lower than 0.5, mainly because negative photochemical production leads to due to NO titration of ozone under high NO_x emissions (NOx-rich conditions). This indicates the control of NOx emissions will benefit ozone reduction during high photochemical pollution period.

3.2.2 Evaluation of impacts from individual source

Sensitivity analyses were conducted using ozone RSM case HSS6-200 to understand the non-linear impacts of different source changes on surface ozone concentrations. Following other sensitive studies (Yarwood et al, 2005; Koo et al., 2009), we defined the "Ozone response" as the change ratio of ozone to the change ratio of emission ($\frac{\Delta Conc\_O_3}{Conc\_O_3} \Big/ (1 - Emission\_ratio)$), to evaluate the control effects of each source. From RSM results, the "Ozone response" can be calculated in a large range of emission variation (from 10% control to 100% control), as seen in Fig.11.

First, we compared the impact of each source under the baseline emissions of other source, i.e., to calculate the difference between the scenario that one source changes with the scenario that no source changes. As shown in Fig. 11a, ozone responses to the changes of anthropogenic NMVOC (up to 100% control) are positive, with a 15~18% ozone reduction in Beijing and Shanghai, and 25~30% ozone reduction in Guangzhou. The benefit for ozone reduction from both local and regional VOC emission control is always recognizable. Therefore, VOC control can be a more effective choice to reduce ozone if NOx emissions stay at the same level.

Though NOx controls usually benefit to ozone reduction in high ozone episodes as we discussed in last section, different NOx sources affect ozone through different mechanisms. The ozone response to the changes of each source (color columns) in three cities, regional NOx sources are strong contributors to ozone concentration (10~20% ozone sensitivity in three cities), while local NOx emission sources are negative contributor until more stringent control ratio reached (respectively 60%, 90% and 80% control in Beijing, Shanghai and Guangzhou by recalculating of combined control effects of two local NOx emission sources). The reason is that the control of regional NOx could significantly reduce the imported ozone (West et al., 2009), but the control of local NOx has negative effects under VOC-limited regime. These results suggest that local controls can hardly solve regional air quality problem, for example, local NOx emission control will increase local ozone mixing ratio. Synchronic control on VOC and regional emissions must be taken into account.

The non-linear relationship of ozone response to precursor emissions is obvious. With the increase of emission reductions, ozone concentration is more sensitive to precursor emissions, shown as the grey line in Fig. 11a. These results suggest that the effectiveness of NOx emission control is strengthened with stricter control efforts. In addition, the interactions among different sources are obvious, as shown the red line in Fig. 11a. It's obvious that red lines in Fig. 11a (represent synchronic control of all emission sources) are above grey lines (represent sum of

separate control on each source) when over 30% emissions are reduced.

In order to explore the nonlinear effects among different sources, we also compared the impact of each source under the synchronic control of other sources. Synchronic control means that all type of emission sources are controlled by same ratio. The impact of each source under the synchronic control of other sources is evaluated through the difference between the synchronic control scenario of all sources and the scenario that an individual source doesn't change.

As seen in Fig. 11b, the VOC control benefit is decreasing with the strengthening of NOx control level, and the ozone is more sensitive to NOx control under higher control level, compared to VOC emission control. That's because biogenic VOC emission hasn't been controlled, the ozone chemistry changes to NOx-limited regime under high NOx control level. Besides, stricter NOx emission control has higher effects on ozone reduction because of the shift from VOC-limited regime to NOx-limited regime. Compared to Fig.11a, the ozone response to regional NOx emission becomes larger, and the ozone response to local NOx emission changes to positive under higher control level, as seen in Fig. 11b. That indicates the enhancement of future control effectiveness should be considered when assessing the impacts of initial emission control actions, especially for NOx emission control. One example is the control of NOx from power plants. When the NOx emission from power plants was set to zero, the ozone response to other NOx emission has been considerably enhanced, seen in Fig 11c, compared to Fig 11a. The effectiveness of control NOx in other sources are enhanced by 1~2 times. Besides, the minimum emission control ratios to avoid the negative impacts of local NOx control will be reduced from 60% to 40% in Beijing, from 100% to 50% in Shanghai, from 80% to 60% in Guangzhou. Therefore, NOx emission control should be significantly enhanced to reduce the ozone pollution in China.

Responses of ozone burdens to precursor emissions over the PBL (defined as layer 1~10, up to 3000 meters) are shown in Fig. 11d. Compared to the responses of surface concentration (as shown in Fig. 11a), sensitivities of ozone burdens to VOC are smaller in all cities, mainly because

the changes of ozone chemistry in vertical profile. The negative impacts from the NOx emission control of local area sources become weaker. However, the negative impacts from the NOx emission control of power plants are even enlarged in Shanghai, which is because of the changes of ozone responses in different vertical height, as shown in Fig. 12. Sensitivity of ozone to NOx emission in area sources decreases in upper layers but that to power plant NOx emissions are even increasing over the PBL. Sensitivity of ozone to VOC emission decreases from Layer 1 to 12. Dominant sources in upper layers (above Layer 10) are regional NOx emissions. The transitions of local NOx impacts from low layers to upper layers are obvious in three cities, and the negative impacts in lower layers are weakened and positive impacts in upper layers (which contributes to regional air quality) are enhanced when strengthening control efforts. Similarly, the discrepancy between red line (represent synchronic control of all sources) and grey line (represent sum of separate control of each source) indicates the obvious interactions among different sources, especially in Beijing and Shanghai.

3.2.3 Suggestion on control policies to achieve air quality standards

During the simulation period (July 2005), high ozone episodes that violate the National Ambient Air Quality Standards for ozone have been found in three cities, as seen in Fig. 13a. Besides, the downwind rural area usually has higher O_3 mixing ratios than urban area as we discussed in Fig. 8. Analysis on the Beijing surface observed O_3 mixing ratios in seven monitoring sites also indicate O_3 mixing ratios in Dingling (a downwind rural site in Beijing) are on average 10% (up to 60%) higher than other urban sites during polluted period. To guarantee the air quality in both urban and rural area, we choose 80% of the National Ambient Air Quality Standard of China, Class II, which equals to the Class I standard (1-hour maximum less than 160μg m^{-3}, approximately 80 ppb) as our policy target.

RSM allows us to calculate the emission reduction ratio to attain a certain target concentration (i.e., 80ppb, 1-h maximum). In order to attain this target, several optional control

scenarios with various control ranges are designed according to the RSM results (HSS6-200 case). The reduction efforts are different when controlling different sources, as shown in Table 4.

If we only control local NOx emissions, 90%, 95% and 85% reduction of local NOx emissions are necessary for Beijing, Shanghai and Guangzhou, respectively, as seen in option 1. Only control local VOC emission cannot attain the target. If we control both local NOx and VOC emission, compared to option 1, the synchronic control on local VOC emission will only reduce the requirement of local NOx reduction from 90% to 80% in Beijing, or even no changes in Shanghai and Guangzhou. That's because the control effectiveness of VOC emissions is small under strengthened NOx control level, besides the regional contribution is much more significant than local impacts. If we control both local and regional NOx emission, compared to option 1, the synchronic control on regional PP NOx emission in option 3 will reduce the requirement of local NOx reduction from 90%, 95%, and 85% to 80%, 85% and 80% in Beijing, Shanghai and Guangzhou, and the synchronic control on all regional NOx emission will reduce the requirement of local NOx reduction to 75%, 80%, 75% in option 4. Additional synchronic controls on both local and regional VOC emissions are considered in option 5 and 6. The requirements of all emission reduction are 65%, 75% and 70% respectively for Beijing, Shanghai and Guangzhou in option 5. Since power plant are relatively easier to be controlled, in option 6 we assume NOx emissions from power plants will be reduced 80% and emissions of other sources will be reduced 60% and 65% and 60% respectively.

Ozone responses under those control strategies are given by Fig.13a. Obvious control effectiveness is shown during high ozone days, and ozone mixing ratios are reduced to <80 ppb. However, the negative impacts still exist during lower ozone days, especially for option 1, 3 and 4 which only controlled NOx emissions. In order to avoid control risk of ozone enhancement by NOx controls under VOC-limited regime, VOC emissions should be synchronically controlled, as in option 5 and 6. The control effectiveness is noticeable over the region. The comparison of monthly

averaged 1-hour maximal ozone concentration between before-controlled (Fig. 13b) and after option 6-controlled (Fig. 13c) indicates the regional air qualities surrounding three cities get improved significantly.

Due to the atypical meteorological conditions as well as the uncertainties from simulations and predictions (rare public-opened observation data), those strategies are restricted in this case study. The ozone sensitivities may still suffer the uncertainties of emission inventory as we discussed in section 2.1. For example, when NOx reduced by 10% and VOC increased by 100%, it's more likely to have the translation from VOC-limited regime to NOx-limited regime, see the 2-D Isopleths of Ozone in Fig 5a. Therefore, it's quite important for the future work to better understand the precursors' emission inventory, especially for VOC emissions. In addition, the potential growth of activities (e.g. energy consumption and vehicle population) is a big challenge for air quality which requires both more sustainable energy policy and better-planned control strategy in the future.

4. Conclusion

A response surface model for ozone control analysis is successfully developed using CMAQ air quality model. Good performances of RSM prediction are under all levels of ozone mixing ratio in both LHS1_30 and HSS6_200. NEs are within 10% and MNEs are within 1% during leave-one-out cross validation and out-of-sample validation. The stability of RSM with high dimensions (HSS6_200) has been confirmed through 2-D isopleths validation. Through computational experiments, key parameters of ozone RSM development has been tested and determined. The maximum numbers for variables involving in statistical interpolation has better performance if not exceeding 8. Marginal processing applied in sampling (e.g., improving the boundary conditions) is recommended to improve the prediction performance, with MNEs reduced by 50%. However, the optimal number varies in different RSM designs (e.g., different control variables, or target pollutants). This paper only uses an efficient way (i.e., the preliminary

experiment) to understand the prerequisite of a successful RSM experiment in the statistical aspect. The crucial parameters (i.e., variable number and run number) need to be carefully considered when using such a statistical method.

Peak ratio appears to be a useful index to understand the ozone formation in responding to the control of NOx and VOC emissions. Spatial (both horizontal and vertical) and temporal variations must be considered when evaluating the emission control effects. In terms of horizontal distribution, NOx control is usually beneficial for the downwind areas which usually have higher ozone concentrations than urban centers. The control of NOx emission gives considerable benefits in upper layers (over 72~674 meters) which can reduce the downwind transport of ozone. In the analysis of diurnal variations, the control of NOx emissions is likely to be more effective than VOC emissions control during heavily polluted episode. Besides, the comparisons against the indicators of NOy component show that the peak ratio is a robust index as good as NOy but can provide further important indication for the degree to NOx emissions control needed to transition from VOC-limited to NOx-limited regime for ozone control over the NOx-rich urban areas.

Different emission sources affect ozone through different mechanisms. Ozone responses to VOC emission changes are always positive under baseline emissions of other sources. However, the effects of VOC emissions control significantly decrease with strengthening NOx emissions control. Therefore, the control of NOx emissions must be considered jointly with the VOC control to reduce urban local ozone. Regional NOx sources are important contributors to ozone concentration (10~20% ozone sensitivity in Beijing, Shanghai and Guangzhou), while local NOx emission sources are negative contributors at surface because of the NO nitration of ozone under NOx-rich urban areas. However, in the upper layers, sensitivities of ozone response to VOC are lower and the negative impacts from the local NOx in urban areas become weaker compared to the responses of surface concentration. Local controls can not alone resolve the regional ozone issue, and thus synchronized control of VOC and NOx emissions must be taken into consideration.

Strong non-linear relationship is obvious for ozone response to NOx emissions. The effectiveness of NOx emission control increases with strengthening control efforts. Therefore the enhancement of future control effectiveness must be considered when assessing the impacts of baseline emission control actions. Comprehensive control policy on multi-sources at both local and regional level is necessary to mitigate ozone problem in China.

Several control strategies are designed to meet this national ozone standard. Effectiveness of NOx and VOC controls is obvious during high ozone days, and ozone levels can be reduced down to 80 ppb ozone standard. One of the cost-effective strategies is to reduce 80% of NOx emissions from power plants and reduce 60% and 65% and 60% of emissions from other sources in Beijing, Shanghai and Guangzhou, respectively.

Acknowledgements

The study was financially supported by National High Technology Research and Development Program of China (2006AA06A309), Natural Science Foundation of China (20921140095), and the U.S. EPA. The authors thank to Dr. Thomas J. Santner and Dr. Gang Han at Ohio State University for their helps on MperK program; Satoru Chatani from Toyota Central R&D Labs and Litao Wang, Qiang Zhang, Dan Chen at Tsinghua University for helping with emission processing.

References

Amann, M., Bertok, I., Borken, J., Chambers, A., Cofala, J., Dentener, F., Heyes, C., Hoglund, L., Klimont, Z., Purohit, P., Rafaj, P., Schöpp, W., Toth, G., Wagner F., and Winiwarter, W.: A tool to combat air pollution and climate change simultaneously. Methodology report, International Institute for Applied Systems Analysis (IIASA), Laxenburg, Austria, 2008.

Binkowski, F.S. and Roselle, S.J.: Models-3 Community Multiscale Air Quality (CMAQ) Model aerosol component, 1. Model description. Journal of Geophysical Research, 108, 4183, doi:10.1029/2001JD001409, 2003.

Box, G. E. P., and Draper N.: Response Surfaces, Mixtures, and Ridge Analyses, Second Edition of [Empirical Model-Building and Response Surfaces, 1987], Wiley, 2007.

Byun, D.W., and Schere, L.K.: Review of the governing equations,computational algorithms and other components of the models-3 Community Multiscale Air Quality(CMAQ) Modeling System Applied Mechanics Reviews 59,2, 51-77, 2006.

Cohan, D.S., Hakami, A., Hu, Y.T., and Russell, A.G.: Nonlinear response of ozone to emissions: source apportionment and sensitivity analysis. Environmental Science & Technology 39, 6739-6748, 2005.

Cohan, D.S., Tian, D., Hu, Y.T., and Russell, A.G.: Control strategy optimization for attainment and exposure mitigation: case study for ozone in Macon, Georgia. Environmental Management, 38, 451-462, 2006.

Cohan, D.S., Boylan, J.W., Marmur, A., and Khan, M.N.: An integrated framework for multipollutant air quality management and its application in Georgia. Environmental Management 40, 545-554, 2007.

Dunker, A. M., Yarwood, G., Ortmann, J.P. and Wilson, G.M.: Comparison of source apportionment and source sensitivity of ozone in a three-dimensional air quality model, Environmental Science and Technology, 36, 2953-2964, 2002.

ENVIRON.: User's guide to the Comprehensive Air Quality Model with Extensions (CAMx). ENVIRON International Corporation, Novato, CA, 2002.

Fu, J.S., Brill, E.D. Jr, Ranjithan, S.R.: Conjunctive use of models to design cost-effective ozone control strategies, J. Air & Waste Manage. Assoc., 56, 800–809, 2006.

Hakami, A. Odman, M. Talat, Russell, and Armistead G.: High-order, direct sensitivity analysis of multidimensional air quality models, *Environmental Science and Technology*, 37, 2442-2452, 2003.

Hammersley, J.: Monte Carlo methods for solving multivariable problems, Proceedings of the New York Academy of Science, 86, 844-874, 1960.

Heyes, C., Schopp, W., Amann, M., Bertok, I., Cofala, J., Gyarfas, F., Kilmont, Z., Makowski, M., Shibayev, S.: A Model for Optimizing Strategies for Controlling Ground-Level Ozone in Europe; Interim Report IR-97-002/January, International Institute for Applied Systems Analysis, 1997, available at: http://www.iiasa.ac.at/Admin/PUB/Documents/IR-97-002.pdf (last access: November 2010).

Iman, R. L., Davenport, J. M., and Zeigler, D. K.: Latin Hypercube Sampling (Program User's Guide). Technical Report SAND79-1473, Sandia National Laboratories, Albuquerque, NM., 1980.

Jang, J.C., Jeffries, H.E., and Tonnesen, S.: Sensitivity of ozone to model grid resolution-II. Detailed process analysis for ozone chemistry. Atmospheric Environment, 29, 3101e3114, 1995.

Klimont, Z., Cofala, J., Xing, J., Wei, W., Zhang, C., Wang, S., Kejun, J., Bhandari, P., Mathur, R., Purohit, P., Rafaj, P., Chambers, A., and Amann, M.: Projections of SO_2, NOx and carbonaceous aerosols emissions in Asia, Tellus B-Chemical And Physical Meteorology, 61, 602-617, 2009.

Koo, B., G.M. Wilson, R.E. Morris, A.M. Dunker, G.Yarwood: Comparison of Source Apportionment and Sensitivity Analysis in a Particulate Matter Air Quality Model, Environ. Sci. Technol., 43, 6669–6675, 2009.

Lei Y, He, K. B., Zhang Q, and Liu Z. Y.: Technology-Based Emission Inventory of Particulate Matters (PM)from Cement Industry, Chinese Journal of Environmental Science, 29, 2366-2371, 2008.

Li, L., Chen, C. H., Huang C., Huang H. Y., Li Z. P., Fu, S. J., Jang J.C., and Streets, D. G.: Regional Air Pollution Characteristics Simulation of O_3 and PM_{10} over Yangtze River Delta Region, Chinese Environmental Science, 29 (1), 237-45, 2008.

Liu, X.H., Zhang, Y., Xing, J., Zhang, Q., Streets, D. G., Jang, C. J., Wang, W.X., and Hao, J.M.: Understanding of Regional Air Pollution over China using CMAQ - Part II. Process Analysis and Ozone Sensitivity to Precursor Emissions, Atmos. Environ., 44, 3719-3727, 2010.

Milford, J.B., Russell, A.G., and McRae, G.J.: A New Approach to Photochemical Pollution Control: Implications of Spatial Patterns in Pollutant Responses to Reductions in Nitrogen Oxides and Reactive Organic Gas Emissions, Environ. Sci. Technol., 23, 1989.

Ohara, T., Akimoto, H., Kurokawa, J., Horii, N., Yamaji, K., Yan, X., and Hayasaka, T.: An Asian emission inventory of anthropogenic emission sources for the period 1980–2020, Atmos. Chem. Phys., 7, 4419-4444, 2007.

Ran, L., Zhao, C., Geng, F., Tie, X., Tang, X., Peng, L., Zhou, G., Yu, Q., Xu, J., and Guenther, A.: Ozone photochemical production in urban Shanghai, China: Analysis based on ground level observations, J. Geophys. Res., 114, D15301, doi:10.1029/2008JD010752, 2009.

Santner, T.J., Williams, B.J. and Notz, W.: The Design and Analysis of Computer Experiments, Springer Verlag, New York, 2003.

Seinfeld, J. H., and Pandis, S.N.: Atmospheric chemistry and physics: From air pollution to climate change, 241 pp., John Wiley and Sons, Inc., 2006.

Shao, M., Tang, X., Zhang, Y., and Li, W., City clusters in China: air and surface water pollution. Frontiers in Ecology & the Environment 4, 353–361, 2006.

Shao, M., Zhang, YH, Zeng, L.-M., Tang, X.-Y., Zhang, J., Zhong, L.-J., and Wang, B.-G.: Ground-level ozone in the Pearl River Delta and the roles of VOC and NOx in its production, JOURNAL OF ENVIRONMENTAL MANAGEMENT 90, 512-518, 2009.

Shih, J.S., Russell, A.G., and McRae, G.J.: An optimization model for photochemical air pollution control, European Journal of Operational Research, 106, 1-14, 1998.

Sillman, S.: The use of NOy, H2O2, and HNO3 as indicators for ozone-NOx-hydrocarbon sensitivity in urban locations. J. Geophys. Res., 100 (D7), 4175-4188. 1995.

Streets, D. G., Bond, T. C., Carmichael, G. R., Fernandes, S. D., Fu,Q., He, D., Klimont, Z., Nelson, S. M., Tsai, N. Y., Wang, M.Q., Woo, J.-H., and Yarber, K. F.: An inventory of gaseous and primary aerosol emissions in Asia in the year 2000, J. Geophys.Res., 108, 8809, 2003

Streets, D.G., Fu, J.S., Jang, C.J., Hao, J.M., He, K.B., Tang, X.Y., Zhang, Y.H., Wang, Z.F., Li, Z.P., Zhang, Q., Wang, L.T., Wang, B.Y., Yu, C.: Air quality during the 2008 Beijing Olympic Games. *Atmospheric Environment* 41, 480-492, 2007

Tang, G., Li, X., Wang, Y., Xin, J. and Ren, X.: Surface ozone trend details and interpretations in Beijing, 2001–2006, Atmos. Chem. Phys., 9, 8813–8823, 2009

Tie, X.-X., Geng, F.-H., Peng, L., Gao, W., and Zhao, C.-S.: Measurement and modeling of O3 variability in Shanghai, China: Application of the WRF-Chem model. Atmospheric Environment 43, 4289-4302, 2009.

Tonnesen, G.S., and Dennis, R.L.: Analysis of radical propagation efficiency to assess ozone sensitivity to hydrocarbons and NOx 1. Local indicators of instantaneous odd oxygen production sensitivity. *Journal of Geophysical Research* 105 (D7), 9213-9225, 2000.

U.S. Environmental Protection Agency: Technical Support Document for the Proposed Mobile Source Air Toxics Rule: Ozone Modeling, Office of Air Quality Planning and Standards, Research Triangle Park, NC, 2006a.

U.S. Environmental Protection Agency: Technical Support Document for the Proposed PM NAAQS Rule: Response Surface Modeling, Office of Air Quality Planning and Standards, Research Triangle Park, NC, 2006b.

Wang, H., Zhou, L. And Tang, X : Ozone concentrations in rural regions of the Yangtze Delta in China. J. Atmos. Chem. 54, 255–265, 2006a.

Wang, T., Ding, A.J., Gao, J., Wu, and W.-S.: Strong ozone production in urban plumes from Beijing, China. Geophys. Res. Lett. 33, L21806, doi:10.1029/2006GL027689, 2006b.

Wang, Z., Li, J., Wang, X., Pochanart, P., and Akimoto, H.: Modeling of regional high ozone episode observed at two mountain sites (Mt. Tai and Huang) in East China. J. Atmos. Chem., 55, 253–272, 2006c.

Wang, X.S, Li, J.-L., Zhang, Y.H., Xie, S.D. and Tang X.Y.: Ozone source attribution during a severe photochemical smog episode in Beijing, China. SCIENCE IN CHINA, 39-6, 548-559, 2009.

Wang, L.H. and Milford, J.B.: Reliability of optimal control strategies for photochemical air pollution. Environ. Sci. Technol., 35, 1173-1180, 2001.

Wang, L.T., Hao, J.M., He, K.B., Wang, S.X., Li, J.H., Zhang, Q., Streets, D.G., Fu, J.S., Jang, C.J., Takekawa, H., Chatani, S.: A Modeling Study of Coarse Particulate Matter Pollution in Beijing: Regional Source Contributions and Control Implications for the 2008 Summer Olympics. J. Air & Waste Manage. Assoc., 58, 1057-1069, 2008.

Wang, L.T., Jang, C., Zhang, Y., Wang, K., Zhang, Q., Streets, D., Fu, J., Lei, Y., Schreifels, J., He, K.B., Hao, J.M., Lam, Y.F., Lin, J., Meskhidze, N., Voorchees, S., Evarts, and D., Phillips, S.: Assessment of air quality benefits from national air pollution control policies in China. Part I: Background, emission scenarios and evaluation of meteorological predictions, Atmospheric Environment, 44, 3442-3448, 2010a.

Wang, S. X., Zhao, M., Xing, J., Wu, Y., Zhou, Y., Lei, Y., He, K. B., Fu, L. X., and Hao, J. M.: Quantifying the Air Pollutants Emission Reduction during the 2008 Olympic Games in Beijing. Environ. Sci. Technol., 44 (7), 2490–2496. DOI: 10.1021/es9028167, 2010b.

Wei, W., Wang, S. X., Chatani, S., Klimont, Z., Cofala, J. and Hao, J. M.: Emission and speciation of non-methane volatile organic compounds from anthropogenic sources in China. Atmospheric Environment, 42 (20), 4976-4988, 2008.

West, J.J., Naik, V., Horowitz, L.W. and Fiore, A.M.: Effect of regional precursor emission controls on long-range ozone transport – Part 1: Short-term changes in ozone air quality. Atmos. Chem. Phys., 9, 6077-6093, 2009.

Xing, J., Wang, S.X., Chatani., S., Cofala, J., Klimont, Z., Amann, M., and Hao, J.M.: Validating Anthropogenic Emissions of China by Satellite and Surface Observations, submitted to Atmospheric Environment, 2010.

Xu, J., Zhang, Y.H., Fu, J. S., Zheng, S.Q., and Wang, W.: Process analysis of typical summertime ozone episodes over the Beijing area. Science of the total environment 399, 147-157, 2008.

Yarwood, G., G. Wilson, R. Morris: DEVELOPMENT OF THE CAMx PARTICULATE SOURCE APPORTIONMENT TECHNOLOGY (PSAT), final report, ENVIRON International Corporation, 2005

Zhang, Y., Vijayaraghavan, K., and Seigneur, C.: Evaluation of Three Probing Techniques in a Three-Dimensional Air Quality Model, *J. Geophys. Res.*, 110 (D02305), doi: 10.1029/2004JD005248., 2005.

Zhang, Y.H., Huang, W., London, S.J., Song, G.X., Chen, G.H., Jiang, L.L., Zhao, N.Q., Chen, B.-H., and Kan, H.-D.: Ozone and Daily Mortality in Shanghai, China, Environ Health Perspect 114, 1227-1232, 2006.

Zhang, Y.H., Su, H., Zhong, L.J. , Cheng, Y.F., Zeng, L.M., Wang, X.S., Xiang, Y.R., Wang, J.L., Gao, D.F., Shao, M., Fan, S.J., and Liu, S.C.: Regional ozone pollution and observation-based approach for analyzing ozone–precursor relationship during the PRIDE-PRD2004 campaign, Atmospheric Environment 42, 6203–6218, 2008.

Zhang, Q., Streets, D. G., Carmichael, G. R., He, K. B., Huo, H., Kannari, A., Klimont, Z., Park, I. S., Reddy, S., Fu, J. S., Chen, D., Duan, L., Lei, Y., Wang, L. T., and Yao, Z. L.: Asian emissions in 2006 for the NASA INTEX-B mission, Atmos. Chem. Phys., 9, 5131-5153, doi:10.5194/acp-9-5131-2009, 2009a.

Zhang, Y., Wen, X.Y., Wang, K., Vijayaraghavan, K., and Jacobson, M.Z.: Probing into Regional O_3 and PM Pollution in the U.S., Part II. An Examination of Formation Mechanisms through a Process Analysis Technique and Sensitivity Study. *J. Geophys. Res.*, 114(D22305), doi:10.1029/2009JD011900, 2009b.

Zhao, Y., Wang, S. X., Duan, L., Lei, Y., Cao, P. F., and Hao, J. M.: Primary air pollutant emissions of coal-fired power plants in China: Current status and future prediction, Atmospheric Environment, 42, 8442-8452, 2008.

Zhao, Y., Nielsen, C.P., Lei, Y., McElroy, M.B., and Hao. J.M.: Quantifying the uncertainties of a bottom-up emission inventory of anthropogenic atmospheric pollutants in China, Atmos. Chem. Phys. Discuss., 10, 29075-29111, 2010

Zheng, J., Zhang L. J., Che, W. W, Zheng, Z. Y., and Yin, S. S.: A highly resolved temporal and spatial air pollutant emission inventory for the Pearl River Delta region, China and its uncertainty assessment, Atmospheric Environment, 43, 5112–5122, 2009.

Table 1 Summary of National Emissions in China in 2005 (units, kt/year)

	SO_2	NOx	PM_{10}	$PM_{2.5}$	BC	OC	NH_3	VOC	
Power Plants	15826	6965	1851	1024	49	20	1	295	
Industrial Combustion	7060	3272	2787	1828	314	146	5	-	-
Industrial Processes	2864	1824	6829	4368	297	251	173	5779	
Cement	1321	1282	4829	3083	18	31	-		-
Iron	931	212	432	317	3	23	-		-
Domestic sources	2458	1335	5220	4656	749	2486	96	1586	
Biofuel	529	559	4388	4251	623	2415	94		-
Transportation	387	4763	441	326	140	138	2	5601	
Others	56	340	2110	2044	46	453	16279	6054	
Open Biomass Burning	56	340	2110	2044	46	453	14		5871
Livestock Farming	-	-	-	-	-	-	7161		-
Mineral Fertilizer Application	-	-	-	-	-	-	8354		-
National total emissions	28651	18499	19237	14245	1595	3494	16556	19406	

Table 2 Sample methods and key parameters used for ozone response surface establishment

RSM case	Variable	Sample method	Sample number
LHS1-30	Total-NOx and Total-VOC	Latin Hypercube Sampling without margin process	30
HSS6-200	Region A* NOx in Power plants; Region A NOx in Area sources; Region A VOC; Region B NOx in Power plants; Region B NOx in Area sources; Region B VOC;	Hammersley quasi-random Sequence Sample with margin level as 6	200

*Region A: Three cities as Beijing, Shanghai and Guangzhou; Region B: Other areas over domain 2

Table 3 Normalized errors of RSM predicted daily 1-hour maximal ozone mixing ratio compared to that simulated by CMAQ through out-of-sample validation, %

	Emission Ratio		Beijing		Shanghai		Guangzhou		East China	
No	NOx	VOC	LHS1-30	HSS6-200	LHS1-30	HSS6-200	LHS1-30	HSS6-200	LHS1-30	HSS6-200
1	0.1	1	2.0	-2.5	1.8	-3.6	-1.5	-0.7	-0.9	-0.2
2	0.3	1	3.2	-1.4	0.5	-2.0	-0.3	-0.2	-1.6	0.1
3	0.5	1	2.8	1.3	-1.0	0.0	0.1	-0.1	-1.5	0.0
4	0.7	1	2.3	1.6	-0.9	1.1	-0.2	0.5	-1.6	-0.8
5	1.5	1	-1.3	-0.4	0.5	-0.5	0.3	0.4	-0.3	-0.2
6	1.9	1	-3.9	-0.2	-1.0	-0.6	-0.1	-0.3	-0.2	0.0
7	1	0.1	0.3	-2.0	0.9	-1.0	-0.6	0.3	-0.1	-1.2
8	1	0.3	0.7	-1.4	0.8	-0.8	0.0	0.5	0.0	-1.4
9	1	0.5	0.9	-0.9	0.5	-0.9	0.4	0.5	-0.3	-1.5
10	1	0.7	1.0	-0.6	0.1	-1.1	0.3	0.0	-0.3	-1.6
11	1	1.5	1.5	0.0	-0.7	-0.7	0.0	0.2	0.0	-1.4
12	1	1.9	1.7	0.3	-1.3	-0.5	-0.1	0.7	-0.1	-1.1
13	0.1	0.1	1.1	-3.5	0.5	-1.7	-2.0	-1.8	-0.7	-0.6
14	0.3	0.3	3.5	-1.9	1.2	-1.6	-0.5	-1.8	-0.1	-0.1
15	0.5	0.5	2.6	1.0	-0.4	0.6	-0.3	-1.0	0.1	-0.1
16	0.7	0.7	2.2	1.4	-0.1	1.2	-0.2	0.1	-0.1	-0.8
17	1.5	1.5	-0.5	-0.3	0.4	0.0	0.1	0.3	0.2	-0.2
18	1.9	1.9	-2.1	-0.3	-0.8	-0.3	-0.6	0.2	-1.0	0.0
Mean Normalized Error			1.9	1.2	0.7	0.4	0.5	0.5	0.5	0.6
Maximal Normalized Error			3.9	3.5	1.8	2.0	1.8	5.5	1.6	1.8

Table 4 Optional NOx/ VOC emission reduction ratios to meet the National Ambient Air Quality Standard in China for ozone (1-hour maximal concentration, 160 μg/m^3)

Beijing	Local NOx PP	Local NOx Other	Local VOC	Regional NOx PP	Regional NOx Other	Regional VOC
Option 1	90%	90%				
Option 2	80%	80%	80%			
Option 3	80%	80%		80%		
Option 4	75%	75%		75%	75%	
Option 5	65%	65%	65%	65%	65%	65%
Option 6	80%	60%	60%	80%	60%	60%

Shanghai	Local NOx PP	Local NOx Other	Local VOC	Regional NOx PP	Regional NOx Other	Regional VOC
Option 1	95%	95%				
Option 2	95%	95%	95%			
Option 3	85%	85%		85%		
Option 4	80%	80%		80%	80%	
Option 5	75%	75%	75%	75%	75%	75%
Option 6	80%	65%	65%	80%	65%	65%

Guangzhou	Local NOx PP	Local NOx Other	Local VOC	Regional NOx PP	Regional NOx Other	Regional VOC
Option 1	85%	85%				
Option 2	85%	85%	85%			
Option 3	80%	80%		80%		
Option 4	75%	75%		75%	75%	
Option 5	70%	70%	70%	70%	70%	70%
Option 6	80%	60%	60%	80%	60%	60%

Note: Option 1- local NOx control only; Option 2- local sources control only; Option 3- power plants and local NOx control only; Option 4- NOx control only; Option 5- control of all sources; Option 6- maximal control of power plant.

Figure captions

Fig. 1 Key steps in the development of response surface model (Orange lines indicate the preliminary experiment to determine the crucial parameters used to establish RSM)

Fig. 2 Map of the CMAQ/RSM modeling domain and interactions among three cities (Monthly mean of 1-hour daily ozone maxima in July 2005, unit: $\mu g/m^3$)

(a) CMAQ and RSM modeling domain

(b) interactions among three cities (Baseline scenario minus the controlled scenario which zeroed out all emissions in three cities, monthly mean of 1-hour daily ozone maxima in July 2005, unit:ppb)

Fig. 3 Margin processing conducted in sampling

(a) Joint distribution of two individual variables (200samples in [0~1])

(b) Distribution density of weighted mean of 4 variables (equals 4 individual variables respectively multiply the "weight coefficients" which were set to be 1:2:3..:N, with sum as 1, red-point represents sample distribution density, dark-line is the fitting trend-line with 4^{th} power)

Fig. 4 Leave-one-out cross-validation of two RSM-Ozone cases (monthly mean of daily 1-hour maxima Ozone, ppb)

Fig. 5 2-D isopleths validation of HSS6-200

(a) 2-D Isopleths of Ozone from HSS6-200 (monthly mean of daily 1-hour maxima, July 2005, ppb)

(b) Normalized error (equal absolute (HSS6-200 minus LHS1-30) divided by LHS1-30, %)

Fig. 6 Sensitivity of prediction performances to marginal level through computational experiments

(a) quasi-HSS-4vs2 (4 types of NOx with 2 types of VOC sources, 100~160 samples)

(b) quasi-LHS-4vs2 (4 types of NOx with 2 types of VOC sources, 160 samples)

Fig. 7 Sensitivity of prediction performances to sample number and variable numbers through computational experiments

Fig. 8 Ozone chemistry variations in Beijing, Shanghai and Guangzhou (Monthly mean of Ozone, NOy mixing ratio, and Peak ratio during afternoon time, 12:00~17:00, July 2005)

Fig. 9 Vertical profile of peak ratio and ozone mixing ratio in Beijing, Shanghai and Guangzhou (monthly mean of daily 1-hour maxima, July 2005)

Fig. 10 Averaged ozone isopleths for high and lower ozone days in three cities

Fig. 11 Ozone response to the stepped control of individual source in 3 cites. (Ozone response = Change ratio of Ozone / Change ratio of Emission; Red solid lines indicate synchronic control of all sources; Colored columns are ozone response to the changes of each source; Grey solid lines indicate sum of separate control on each source; All values are averaged of 1-hour maxima ozone in high ozone days in July, 2005)

Fig. 12 Vertical profile Ozone response to the stepped control of individual source in 3 cites. (Ozone response = Change ratio of Ozone / Change ratio of Emission; Red solid lines indicate synchronic control on all sources; Colored columns are ozone response to the changes of each source; Grey solid lines indicate sum of separate control on each source; The height of layers 1-14 above ground are 36, 72, 145, 294, 444, 674, 1070, 1568, 2093, 2940, 3991, 5807, 9057, 14648 meters respectively; All values are averaged of ozone during afternoon time, 12:00~17:00 in July, 2005)

Fig. 13 Effectiveness of NOx/VOC control strategies to achieve secondary national ozone standards in 3 cities (daily-maxima, 2005 Jul)

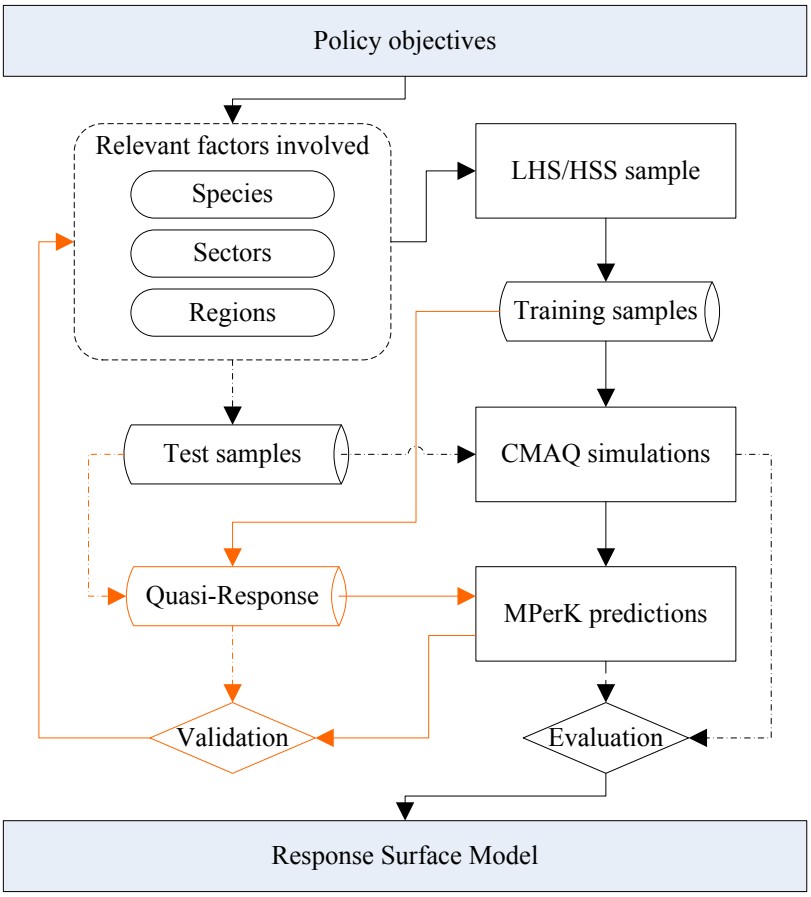

Fig. 1 Key steps in the development of response surface model (Orange lines indicate the preliminary experiment to determine the crucial parameters used to establish RSM)

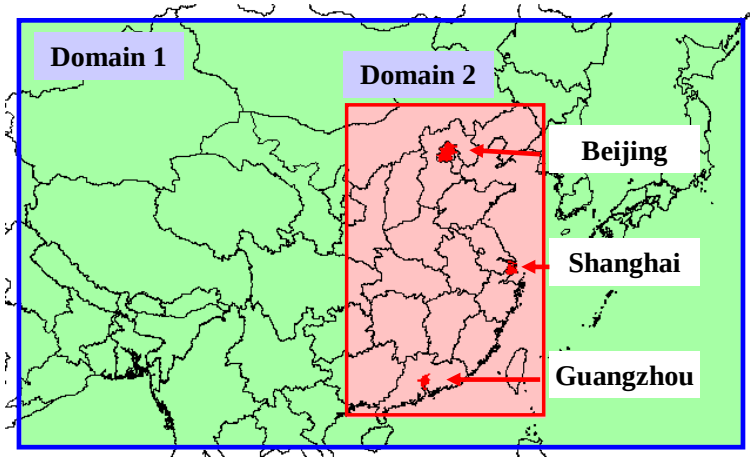

(a) CMAQ and RSM modeling domain

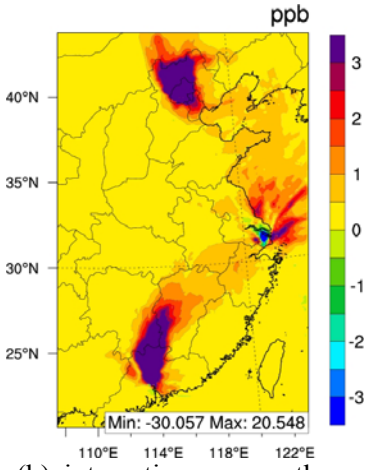

(b) interactions among three cities (Baseline scenario minus the controlled scenario which zeroed out all emissions in three cities, monthly mean of 1-hour daily ozone maxima in July 2005, unit:ppb)

Fig. 2 Map of the CMAQ/RSM modeling domain and interactions among three cities

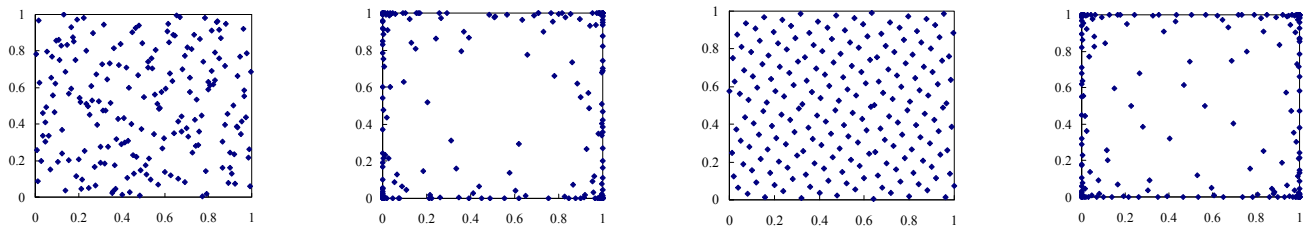

LHS1 LHS6 HSS1 HSS6

(a) Joint distribution of two individual variables (200samples in [0~1])

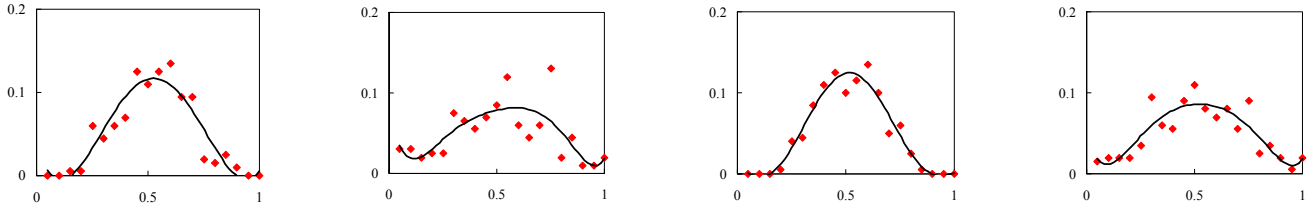

LHS1 LHS6 HSS1 HSS6

(b) Distribution density of weighted mean of 4 variables (equals 4 individual variables respectively multiply the "weight coefficients" which were set to be 1:2:3..:N, with sum as 1, red-point represents sample distribution density, dark-line is the fitting trend-line with 4^{th} power)

Fig. 3 Margin processing conducted in sampling

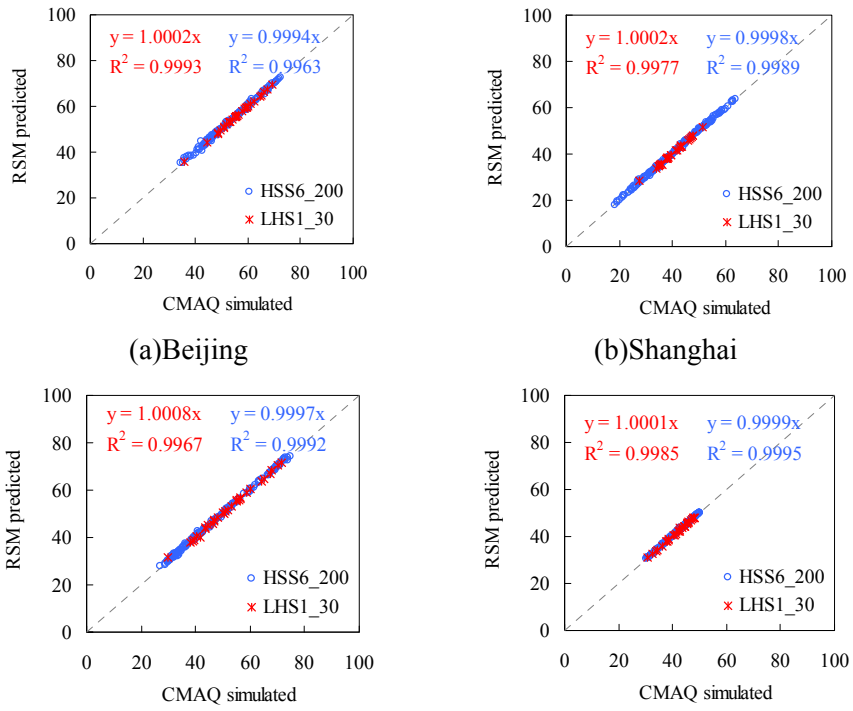

(a)Beijing

(b)Shanghai

(c)Guangzhou

(d)East China

Fig. 4 Leave-one-out cross-validation of two RSM-Ozone cases (monthly mean of daily 1-hour maxima Ozone, ppb)

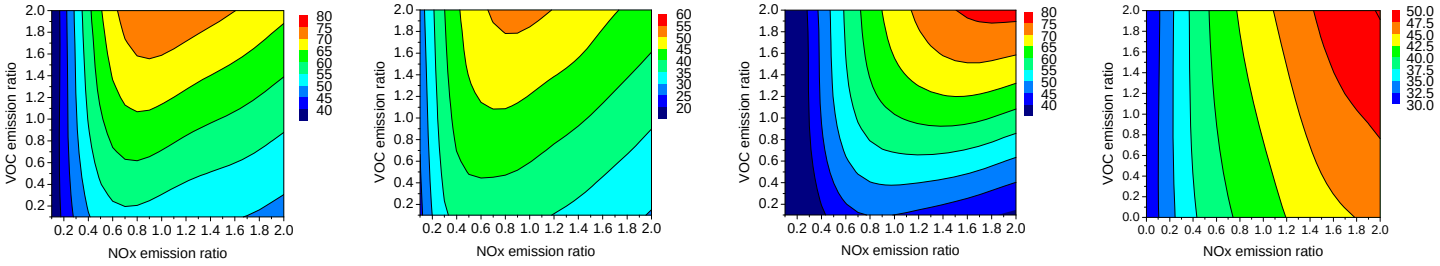

(a) 2-D Isopleths of Ozone from HSS6-200 (monthly mean of daily 1-hour maxima, July 2005, ppb)

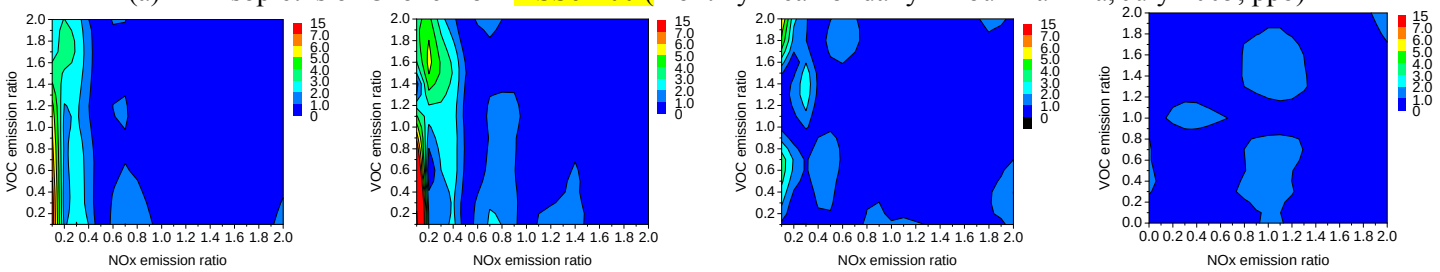

(b) Normalized error (equal absolute (HSS6-200 minus LHS1-30) divided by LHS1-30, %)

Fig. 5 2-D isopleths validation of HSS6-200

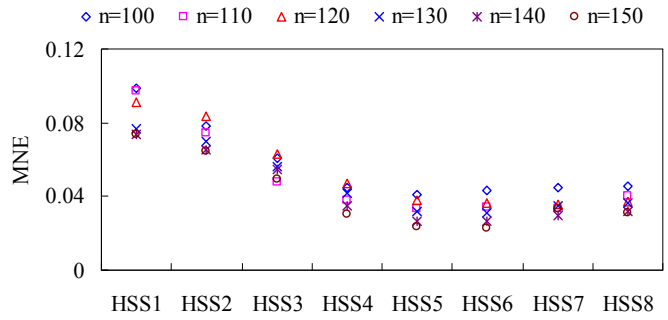

(a) quasi-HSS-4vs2 (4 types of NOx with 2 types of VOC sources, 100~160 samples)

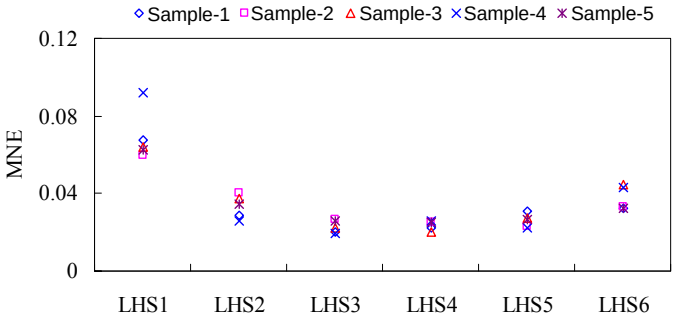

(b) quasi-LHS-4vs2 (4 types of NOx with 2 types of VOC sources, 160 samples)

Fig. 6 Sensitivity of prediction performances to marginal level through computational experiments

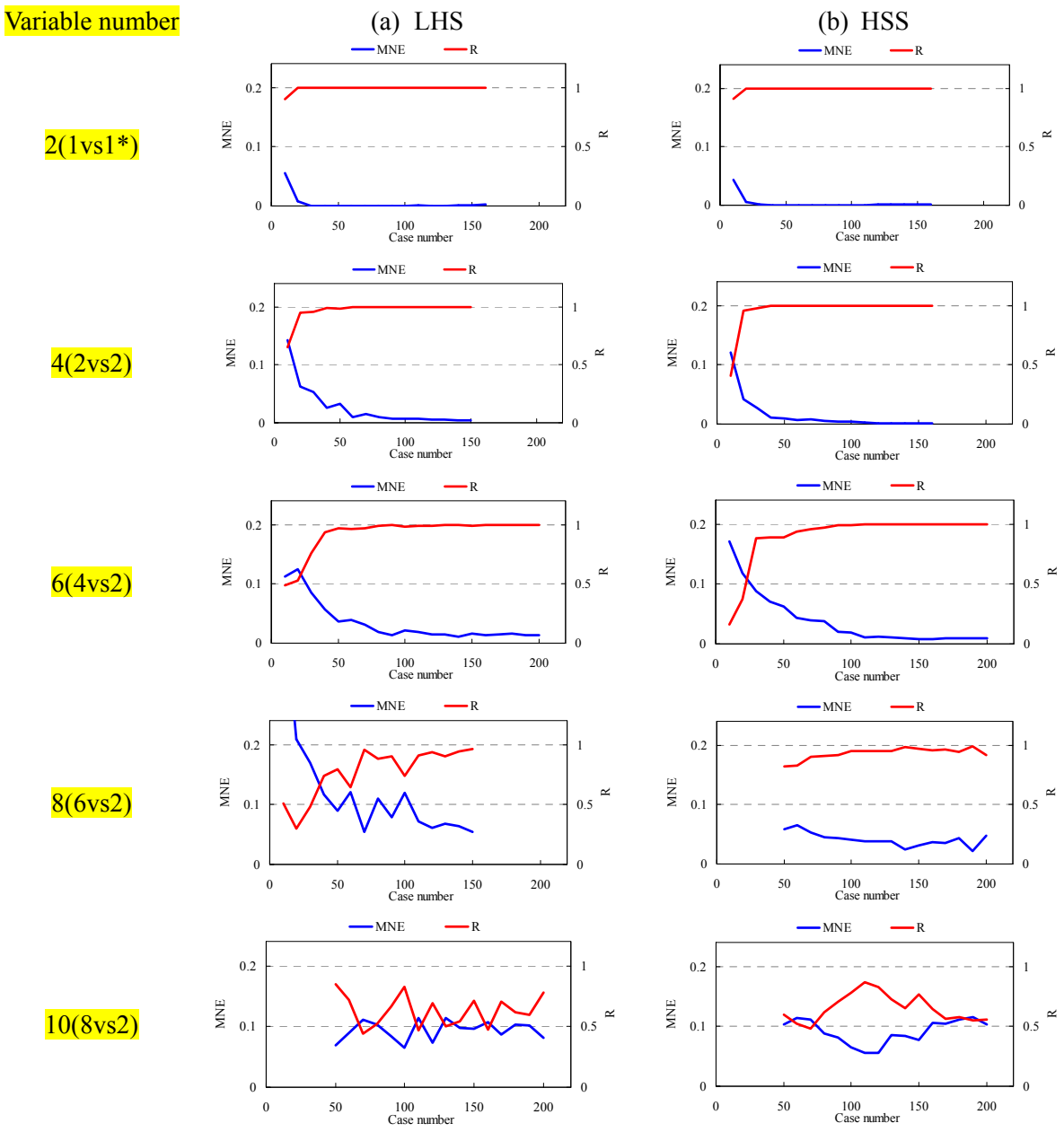

Fig. 7 Sensitivity of prediction performances to sample number and variable numbers through computational experiments (*1vs1 means 1 types of NOx emissions sources and 1 types of VOC emission sources)

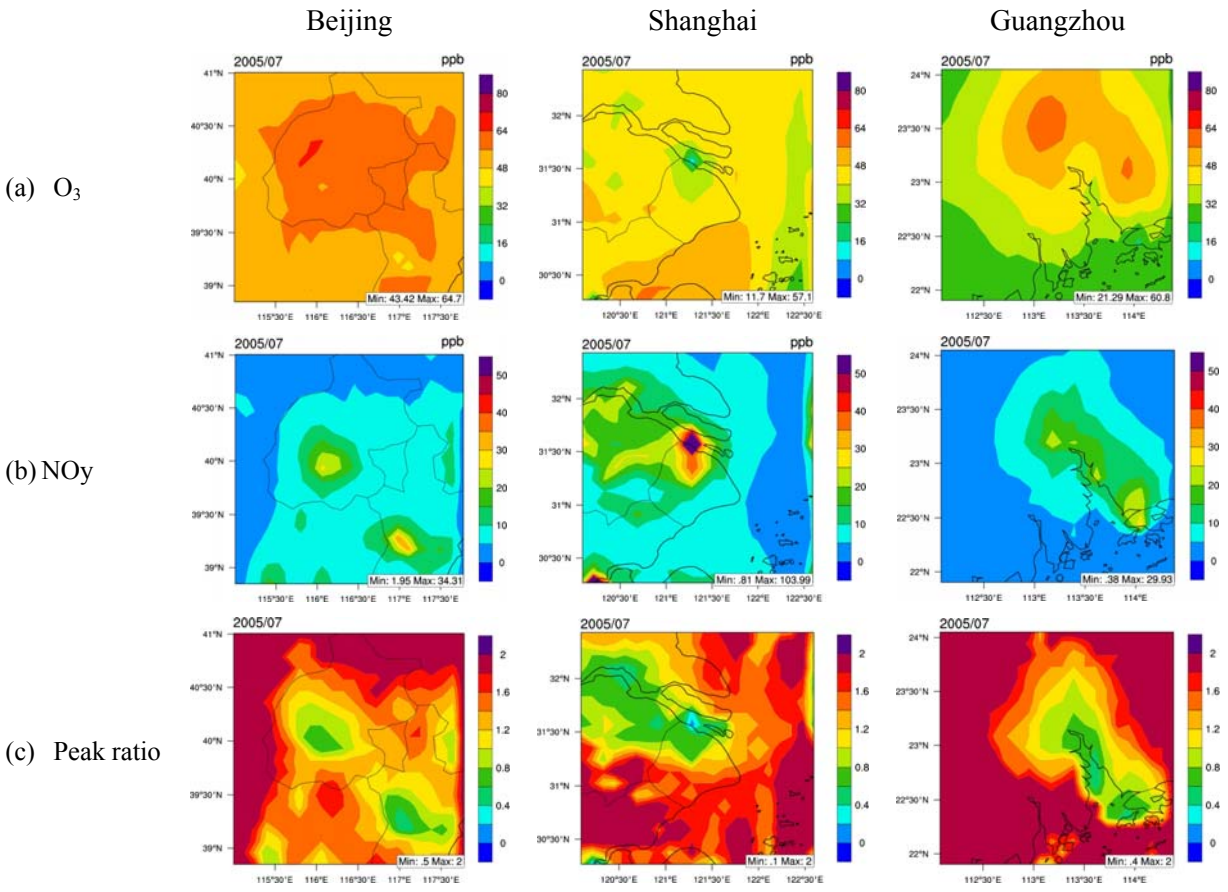

Fig. 8 Ozone chemistry variations in Beijing, Shanghai and Guangzhou (Monthly mean of Ozone, NOy mixing ratio, and Peak ratio during afternoon time, 12:00~17:00, July 2005)

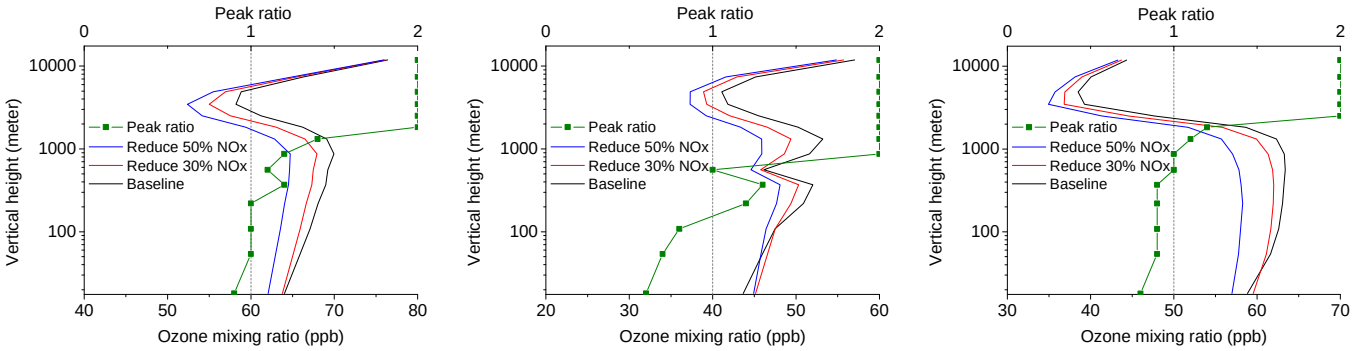

(a) Beijing (b) Shanghai (c) Guangzhou

Fig. 9 Vertical profile of peak ratio and ozone mixing ratio in Beijing, Shanghai and Guangzhou (monthly mean of daily 1-hour maxima, July 2005)

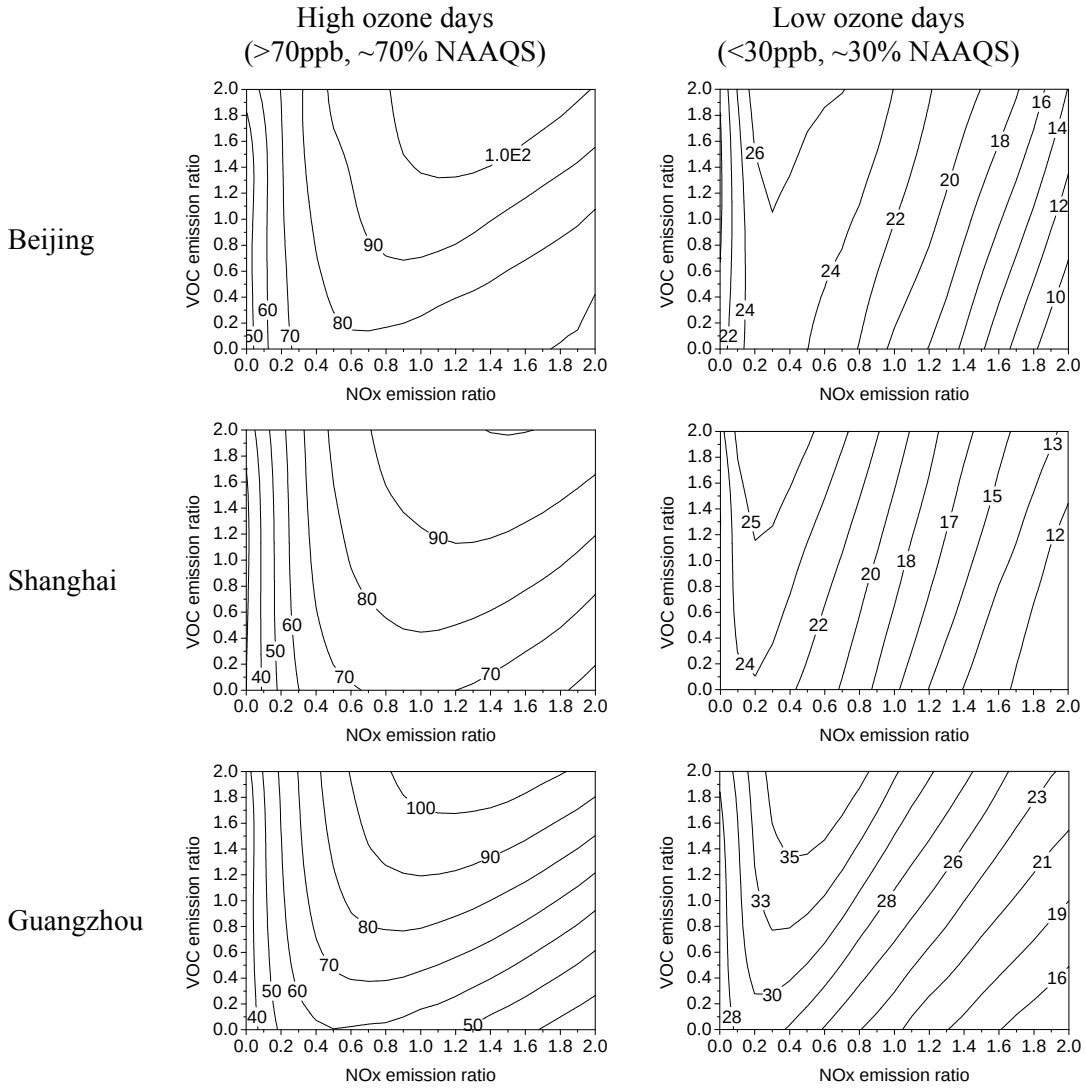

Fig. 10 Averaged ozone isopleths for high and lower ozone days in three cities

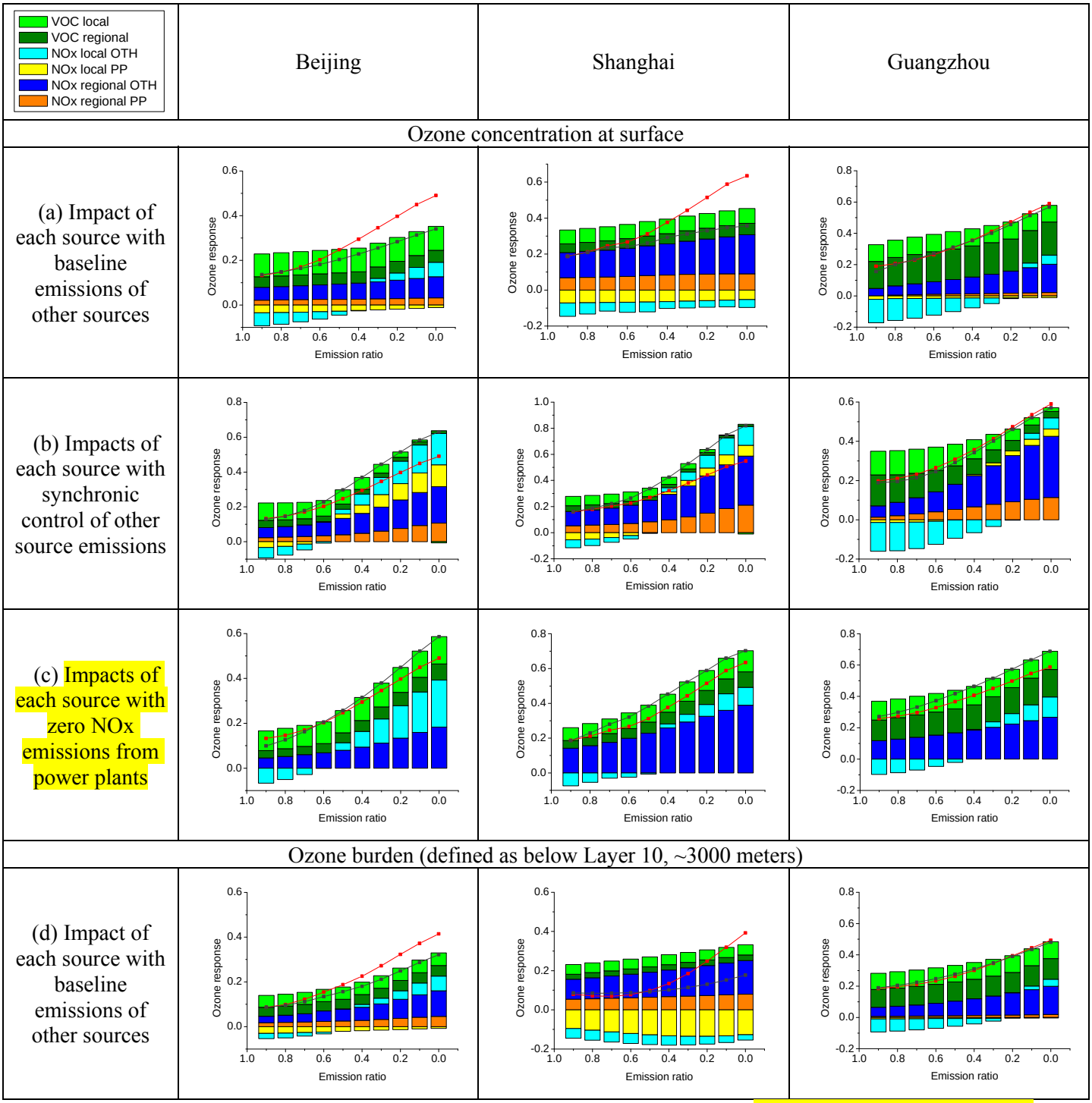

Fig. 11 Ozone response to the stepped control of individual source in 3 cites. (Ozone response = Change ratio of Ozone / Change ratio of Emission; Red solid lines indicate synchronic control of all sources; Colored columns are ozone response to the changes of each source; Grey solid lines indicate sum of separate control on each source; All values are averaged of 1-hour maxima ozone in high ozone days in July, 2005)

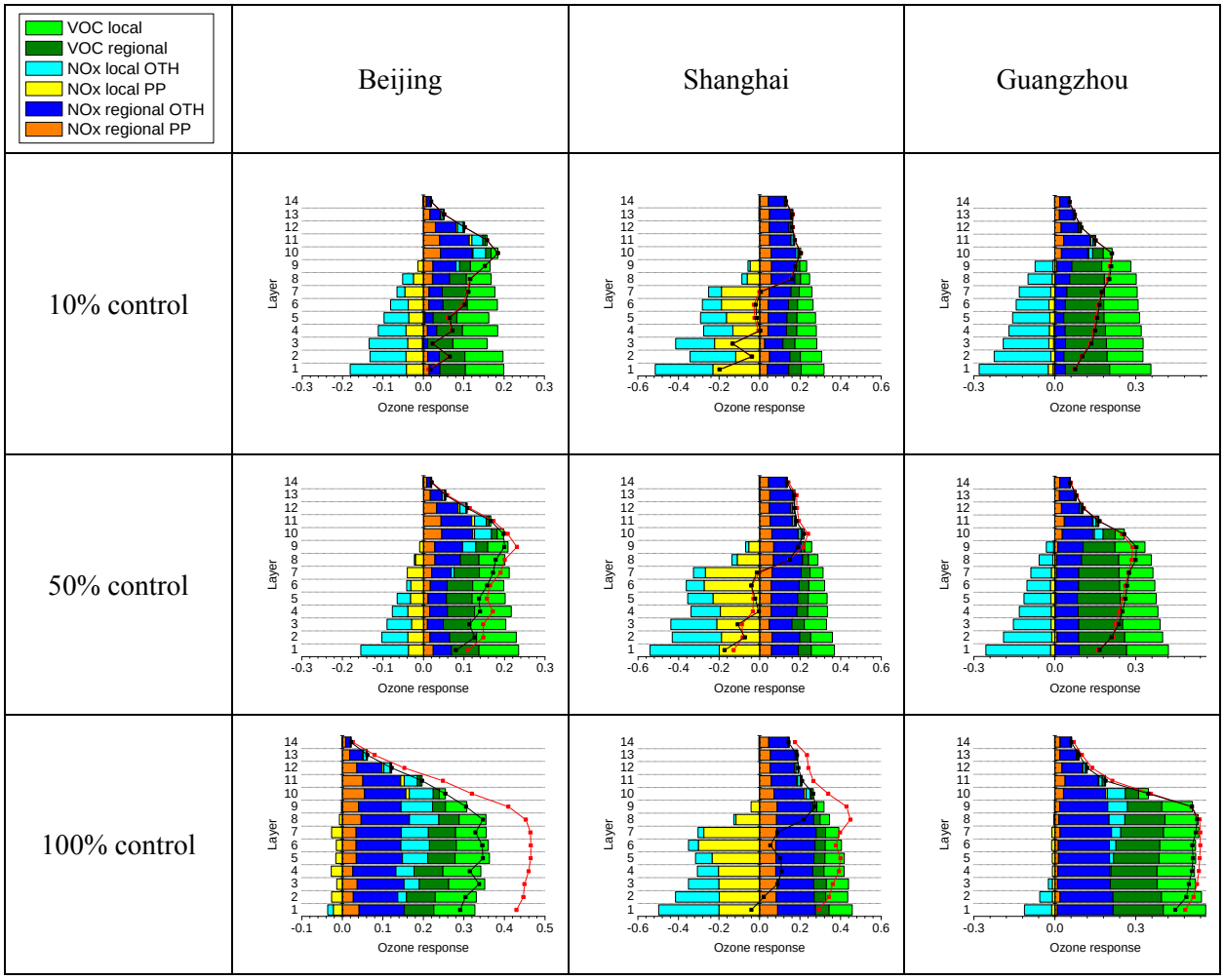

Fig. 12 Vertical profile Ozone response to the stepped control of individual source in 3 cites. (Ozone response = Change ratio of Ozone / Change ratio of Emission; Red solid lines indicate synchronic control on all sources; Colored columns are ozone response to the changes of each source; Grey solid lines indicate sum of separate control on each source; The height of layers 1-14 above ground are 36, 72, 145, 294, 444, 674, 1070, 1568, 2093, 2940, 3991, 5807, 9057, 14648 meters respectively; All values are averaged of ozone during afternoon time, 12:00~17:00 in July, 2005)

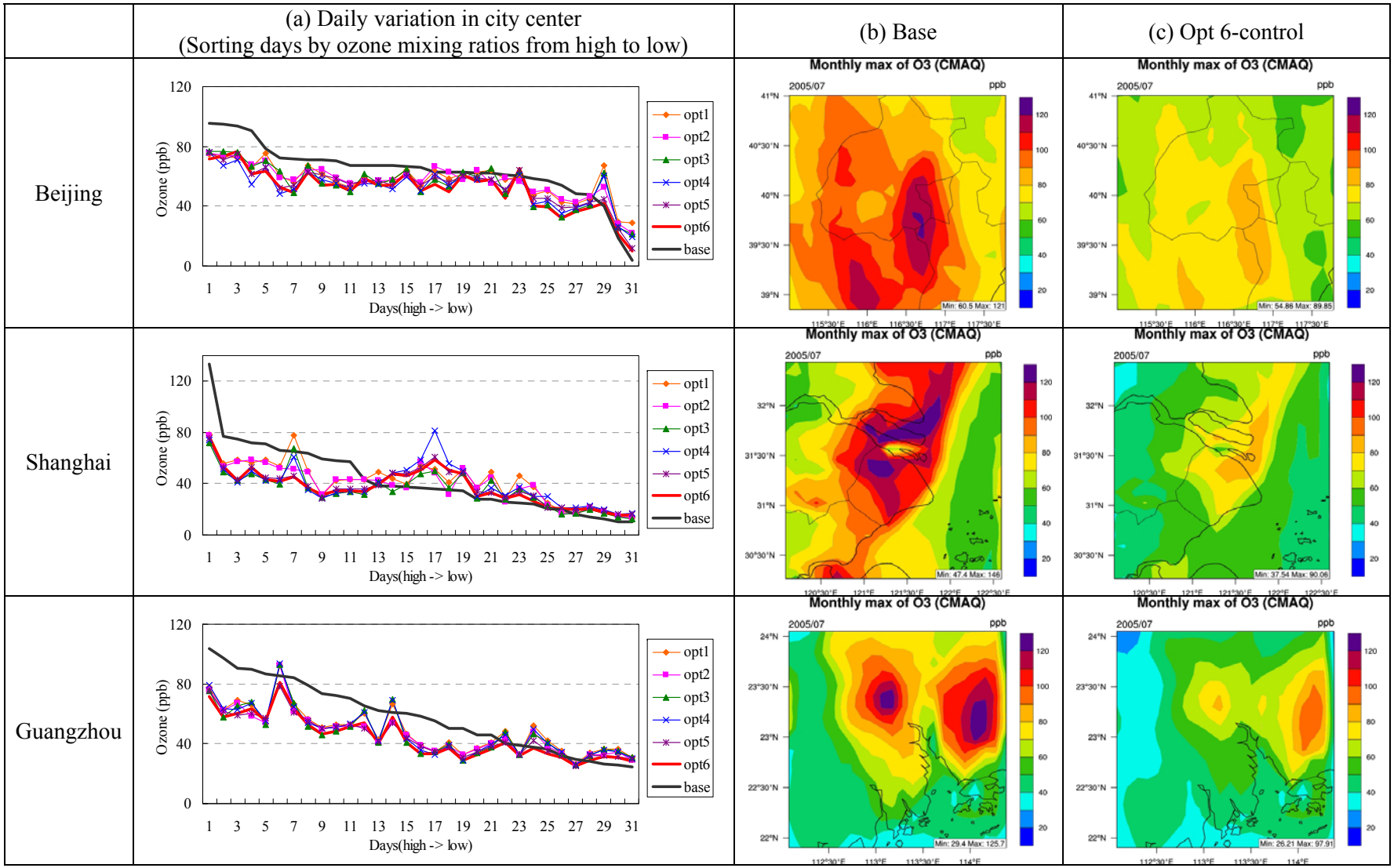

Fig. 13 Effectiveness of NOx/VOC control strategies to achieve secondary national ozone standards in 3 cities (daily-maxima, 2005 Jul)